Int. J. Electrochem. Sci., 15 **(2020)** 10707 – 10721, doi: 10.20964/2020.11.66

International Journal of ELECTROCHEMICAL SCIENCE
www.electrochemsci.org

Cyclic Voltammetric and Spectroelectrochemical Studies of Tris(5-amino-1,10-phenantroline)Iron(II) Polymer Films

Kenneth L. Brown[*]*, Rebecca Danforth, Evan Bleitz, Yechan Hwang and Dustin Rens*

Hope College, Department of Chemistry, Holland, MI 494923
[*]E-mail: brownk@hope.edu

Received: 30 June 2020 / *Accepted:* 8 September 2020 / *Published:* 30 September 2020

Tris(5-amino-1,10-phenantroline)iron(II) polymer films were prepared on glassy carbon electrodes and indium tin oxide (ITO) surfaces using cyclic voltammetry. The cyclic voltammograms collected during electropolymerization are correlated with the electrochemical and spectroelectrochemical characterization observations of the polymer films. On ITO surfaces, the films demonstrate reversible electrochromism switching between colors of red and yellow due to potential changes either in the cyclic voltammetry-scanning potential or pulsed-potential mode. Spectroelectrochemical measurements of the polymer films were made using tetraethyl- and tetrabutyl-ammonium perchlorate supporting electrolyte solutions. The absorbance at 506 nm is significantly diminished when measurements are made in tetrabutylammonium perchlorate supporting electrolyte solutions, indicating that spectroelectrochemical responses are limited by counterion diffusion within the polymer films.

Keywords: Electropolymerization, cyclic voltammetry, spectroelectrochemistry, indium tin oxide, polymer films

1. INTRODUCTION

Redox polymer films and organic conducting polymer films [1-3] have been important components to function as selective reagents in compact, robust, and sensitive electrochemical sensors and biosensors capable of detecting a wide variety of analytes. Cyclic voltammetry still remains a versatile technique used to design polymer films for electrochromic devices for various types of panel displays and electrochemical sensors and biosensors. In addition, these types of polymer films have been used to develop neuroelectrodes and they can prevent corrosion and improve super capacitors [4-6]. Although this method is effective for immobilizing compounds to an electrode surface, the polymer film does not necessarily grow in regular layers, and hence, electrode surface coverage may require several thousand monolayers to achieve complete surface coverage. This technique, under specified

experimental conditions (e.g., specific scan rates and potential windows), produces polymeric films with consistent molecular architectures, mechanical stabilities, morphologies, and charge-transfer properties [7-11]. Two significant advantages of using polymeric thin films as selective reagents in chemical and electrochemical sensing are the ability to (1) improve control over the chemical and physical nature of the reaction system and (2) provide a much higher effective "concentration density" for reactions to occur. Spectroelectrochemistry offers the advantage of simultaneously probing the electrochemical and optical properties of compounds affixed to transparent electrodes. Several groups have exploited this hyphenated technique to develop flexible electrochromic materials and spectroelectrochemical sensors [12, 13]. Meanwhile, electrochemical impedance spectroscopy (EIS) is a versatile technique used to characterize and differentiate between mass transport and charge transfer reactions occurring at electrode surfaces of redox species in solution and chemically modified electrodes. Different types of diffusion, such as finite, semi-infinite, and infinite, which is based on the time scale of the electrochemical experiment and thickness of the film, can impact the overall electrochemical response of materials confined to surfaces when electrochemically stimulated [14, 15]. The diffusional fluxes of ions within the polymer film will give rise to a Warburg impedance that is dependent upon the frequency of perturbation. We have used EIS to better understand the charge transfer dynamics of tris(5-amino-1,10-phenanthroline)iron(II) [Fe(Phen-NH_2)$_3$] polymer films and to determine the role of diffusion within these polymer films.

Tris(5-amino-1,10-phenanthroline)iron(II) electropolymerized films have been studied by several research groups [16, 17] and have been used as redox mediators in glucose biosensors. However, to date, no extensive study has been made on the spectroelectrochemical and electrochromic properties of electropolymerized films derived from this compound. Furthermore, few applications of using this compound in electrochemical systems have been noted. Therefore, in the development of spectroelectrochemical sensors, we have revisited the electrochemical and spectroelectrochemical properties of Fe(Phen-NH_2)$_3$ polymer films. In addition, atomic force microscopy and scanning electron microscopy were used to study the morphological and optical properties of the electropolymerized films on ITO surfaces.

2. EXPERIMENTAL

2.1 Reagents and Solutions.

Tris(5-amino-1,10-phenanthroline)iron(II) was synthesized according to procedures published by Neils and researchers with no changes therein [17]. WebMO Basic computational software interfaced with the Windows 10 operating system was used to build a computer model of [Fe(Phen-NH_2)$_3$]. Acetonitrile, used as a solvent in all solutions, was purchased from Sigma Aldrich (St. Louis, MO). Solutions of the iron complex were maintained at 1.00 x 10^{-3} M in 0.100 M tetraethylammonium perchlorate (TEAP). Residual amounts of water in the electropolymerization solution compromises the ability to successfully form the polymer film, as the residual water lowers the solubility of the iron complex. As a result, prior to using TEAP or TBAP, which were obtained from GFS Chemicals

(Powell, OH), the salts were dried under vacuum to remove the residual water and stored in a desiccator until use. Glassy carbon electrode polishing and ITO surface cleaning are described elsewhere [2].

2.2 Procedure for electropolymerization on glassy carbon electrodes and ITO surfaces and cyclic voltammetric and EIS characterization of poly-Fe(Phen-NH_2)$_3$ films.

All electrochemical measurements were made using a CHInstruments (Austin, TX) or a PalmSens (UK) potentiostat in a three-electrode cell configuration. The working electrode was either a glassy carbon electrode (0.0706 cm^2) obtained from CHInstruments or an ITO covered glass substrate. The ITO surfaces used for spectroelectrochemical studies had dimensions of 7 mm x 50 mm x 0.6 mm (width, height, and thickness) and were coated on one side of a glass substrate; a resistance of < 10 ohms was obtained with a system from Delta Technologies (Stillwater, MN). A platinum electrode from CHInstruments served as the auxiliary electrode. The reference electrode obtained from Innovative Instruments Inc. (Tampa, FL) was solid-state Ag/AgCl (3.4 M KCl) and leak-free. Electropolymerizations were completed using a scan rate of 100 $mV{\cdot}s^{-1}$ in a potential window of 2.00 V to 0 V. The films on the glassy carbon electrodes and ITO surfaces were characterized at variable scan rates from 10 $mV{\cdot}s^{-1}$ to 100 $mV{\cdot}s^{-1}$ in a potential window of 2.00 V to 0 V in the supporting electrolyte solutions. Impedance measurements were made using glassy carbon electrodes at a DC potential of 1.30 V and an AC amplitude potential of 10 mV vs Ag/AgCl reference electrode using a frequency range of 0.001 Hz-50000 Hz.

2.3 Procedure for spectroelectrochemical and surface studies.

Spectroelectrochemical measurements were made with a Cary 5E UV/VIS/NIR spectrophotometer using a three-electrode cell system in a 1.00-cm glass cuvette. A specially made spectroelectrochemical cell top was designed to accommodate the three-electrode cell in the 1.00-cm glass cuvette. The spectroelectrochemical measurements of the polymer films on ITO surfaces made in the cyclic voltammetry mode at 25 $mV{\cdot}s^{-1}$ (2.00 V to 0 V) and pulse-based mode were based on twenty cycles of electropolymerization on the ITO surface. In the pulse-based mode, applied potentials were held for 1 minute at +1.50 V, +1.35 V, +1.30 V, +1.25 V and +1.20 V before a spectrum was obtained for the polymer film. All the measurements were made in 0.100 M TEAP or 0.100 M TBAP supporting electrolyte solutions. Scanning electron microscopy measurements were made using an EM-30 series instrument (Element Precision Imaging). A Dimension Icon atomic force microscope (Bruker, Santa Barbara, CA) was used to obtain the film thickness of the polymer film on the ITO surface.

3. RESULTS AND DISCUSSION

3.1 Electropolymerization of tris(5-amino-1,10-phenanthroline)iron(II) on glassy carbon electrodes.

Figure 1 shows the structure of $Fe(Phen\text{-}NH_2)_3$ drawn using WebMO computational software and cyclic voltammograms corresponding to twenty cycles of the electropolymerization of $Fe(Phen\text{-}NH_2)_3$ on a glassy carbon electrode [18]. Regardless of the working electrode used (i.e., glassy carbon or ITO) the mechanism of forming these films commences with the irreversible oxidation of the amine substituent at 1.18 V on the glassy carbon electrode to produce radical cations that combine at the electrode surface. The coupling reaction is followed by the loss of protons, providing a neutral species. Chain propagation occurs via the addition of more monomer units through radical cation coupling, which causes the insoluble polymeric material to become deposited onto the electrode surface. Other compounds, such as metal(II)-tetraaminophthalocyanines, thiophene, 3,4-ethylenedioxythiophene (EDOT), and aniline, are known to proceed with similar mechanisms to form their corresponding polymer films [10, 19]. However, the peak due to amine oxidation eventually becomes overlapped by the growth of the peak corresponding to $Fe^{2+} \rightarrow Fe^{3+} + e^-$. The main redox reaction, $Fe^{3+} \rightleftharpoons Fe^{2+} + e^-$, produces the anodic peak (E_{pa}) and cathodic peak (E_{pc}) with $E^{o'}$ of 1.25 V (glassy carbon electrode), where $E^{o'}$, the formal reduction potential, is the average of the E_{pc} and E_{pa} peak potentials. The increase in the peak currents during electropolymerization results from the accumulated monolayers deposited on the electrode surface and increased surface area related to the changing surface roughness.

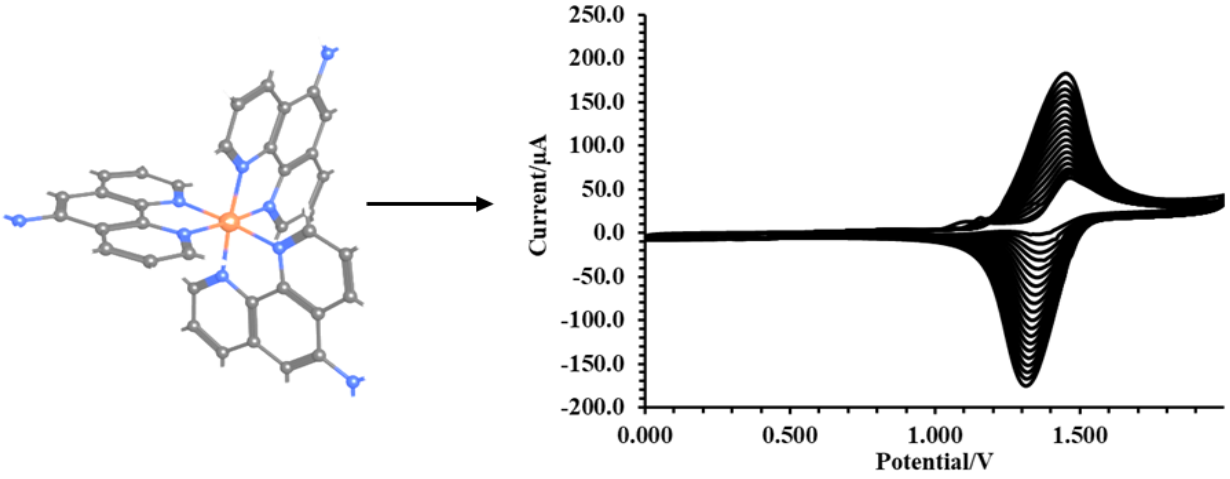

Figure 1. The structure of $Fe(Phen\text{-}NH_2)_3$ and twenty cycles of the electropolymerization of 1.00 x 10^{-3} M $Fe(Phen\text{-}NH_2)_3$ in 0.100 M TEAP at 100 $mV \cdot s^{-1}$ using a potential of 0.00 V to 2.00 V vs Ag/AgCl are shown.

Figure 2 shows an overlay of the cyclic voltammograms corresponding to cycles one and twenty on a glassy carbon electrode. The peak separation of the $Fe^{2+/3+}$ redox couple during electropolymerization varies from 0.090 V to 0.110 V on glassy carbon electrodes. At the onset of electropolymerization, the ratio of the peak currents (i_{pa}/i_{pc}) is 1.53, but afterwards, this ratio is 0.990-1.09.

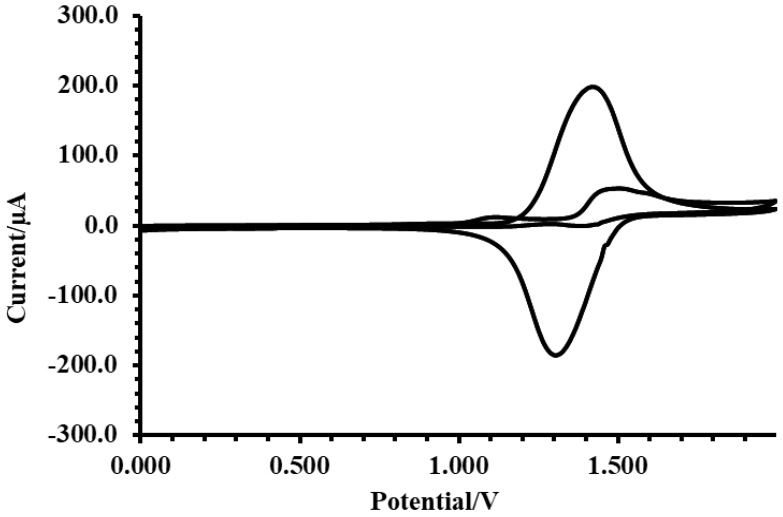

Figure 2. The differences between cycle one and cycle twenty are shown for the electropolymerization of Fe(Phen-NH_2)$_3$ on a glassy carbon working electrode. Solution conditions are the same as in Figure 1.

Figure 3a shows an overlay of the cyclic voltammograms from 75 mV·s^{-1} to 275 mV·s^{-1}. The diagnostic plots shown in Figure 3b of the peak currents with respect to the square root of the scan rate from 75 to 300 mV·s^{-1} are linear according to the Randles-Sevcik equation, $i_p = 2.69 \times 10^5 n^{3/2} A C D^{1/2} \nu^{1/2}$, indicating diffusion-controlled mass transport conditions during the electropolymerization process [20]. The symbols have their common electrochemical representation.

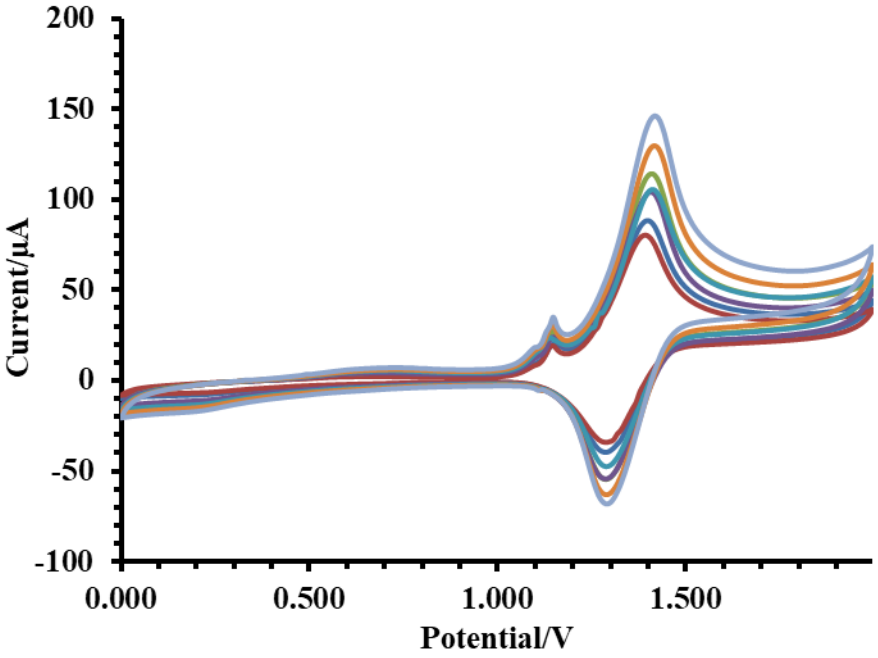

Figure 3a. The overlay of the cyclic voltammograms of the electropolymerization of 1.00 x 10^{-3} M Fe(Phen-NH_2)$_3$ in 0.100 M TEAP conducted at scan rates from 75 to 275 mV·s^{-1} using a potential of 0.00 V to 2.00 V vs Ag/AgCl.

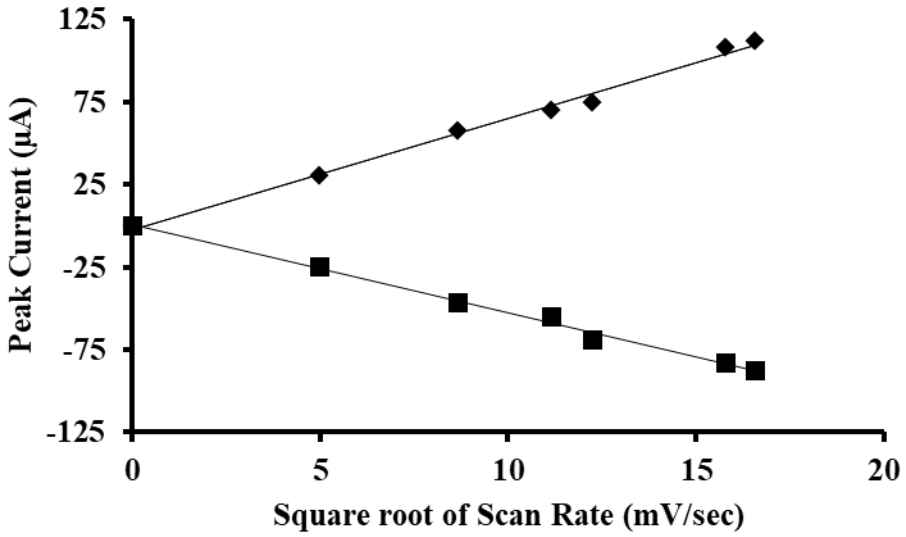

Figure 3b. A plot of the peak currents with respect to the square root of the scan rates from 75 to 275 $mV \cdot s^{-1}$, showing the diffusion-controlled conditions for electropolymerization.

3.2 Electropolymerization of tris(5-amino-1,10-phenanthroline)iron(II) on indium tin oxide surfaces.

The electropolymerization of $Fe(Phen\text{-}NH_2)_3$ on ITO surfaces shown in Figure 4 parallels very closely with the electropolymerization of $Fe(Phen\text{-}NH_2)_3$ on GC electrodes. The initial oxidation of the -amino group occurs at 1.08 V. However, the peak separations of the $Fe^{2+/3+}$ redox couple for each cycle of electropolymerization are much greater than those obtained with the GC electrodes. During the first cycle, the peak separation is 276 mV, whereas on the GC electrode, the peak separation is 90 mV. As the electropolymerization process continues, ΔEp/cycle on ITO surfaces varies linearly from 276 mV to 575 mV. Due to the ohmic resistance, the electrochemistry of $Fe(Phen\text{-}NH_2)_3$ on ITO surfaces shows a more quasi-reversible behavior than that on the glassy carbon electrodes, although the films are formed on the ITO surface with the same ease as the films formed on the glassy carbon electrodes; the peak separation values are relatively constant on GC electrodes.

3.3 Cyclic voltammetric characterization of poly-$Fe(Phen\text{-}NH_2)_3$ films.

Examination of the GC electrodes after electropolymerization revealed a red film that increased in color intensity as the surface coverage increased. When the electrode was rinsed with fresh solvent, placed in the supporting electrolyte solution, 0.100 M TEAP in CH_3CN, and characterized (Figure 5), the cathodic and anodic peaks persisted upon scanning from 2.00 V to 0 V at 25 $mV \cdot s^{-1}$. The $E^{o'}$ value of $Fe^{3+} \rightleftharpoons Fe^{2+} + e^-$ is 1.37 V, which is similar to the $E^{o'}$ value of the $Fe^{3+/2+}$ redox couple obtained during the electropolymerization cyclic voltammetry. A surface coverage of 5.10×10^{-7} mol/cm^2 was determined using the area under the anodic peak. The cathodic and anodic peaks in Figure 5 are the result of several processes: 1) charge transfer at the electrode|polymer interface, 2) electron hopping between nearby redox centers throughout the polymer film, 3) egress or ingress of ions from the film

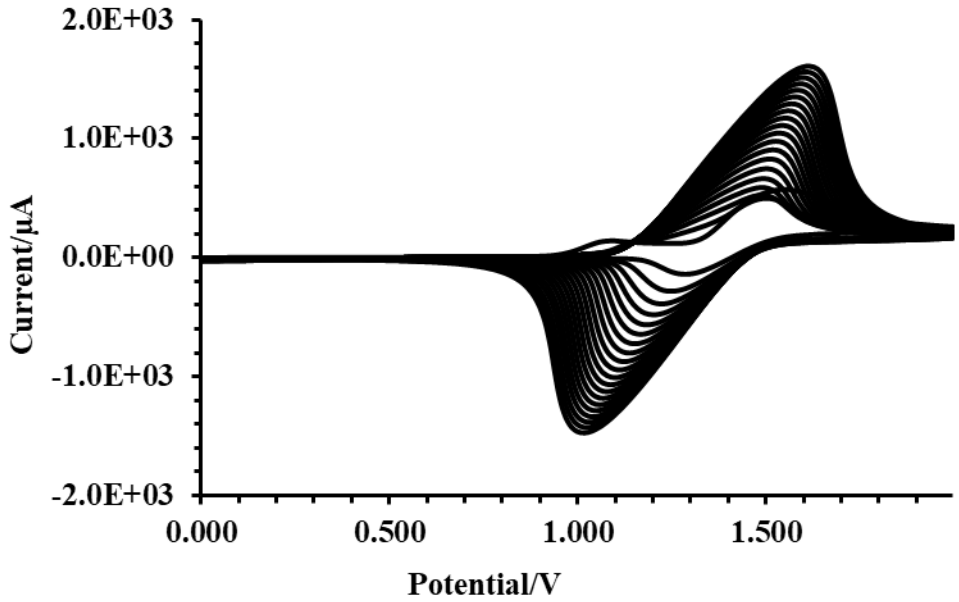

Figure 4. Cyclic voltammogram shows twenty cycles of the electropolymerization of 1.00 x 10^{-3} M Fe(Phen-NH_2)$_3$ in 0.100 M TEAP at 100 mV·s^{-1} using a potential of 0.00 V to 2.00 V vs Ag/AgCl on an ITO surface.

via the electrolyte supporting electrolyte solutions to maintain charge electroneutrality, and 4) possible changes in the polymer network to accommodate charge transfer reactions and ionic movement within the polymer structure [21]. During the oxidation and reduction reactions, solvated counterions enter or leave the polymeric network to maintain charge electroneutrality and may cause the film to swell, thus changing the mechanical integrity of the film [22, 23]. Diagnostic plots of the peak current relative to the scan rate produced linear plots, indicating thin film electrochemistry, wherein finite diffusion dominates the electron transfer process within the films [24, 25].

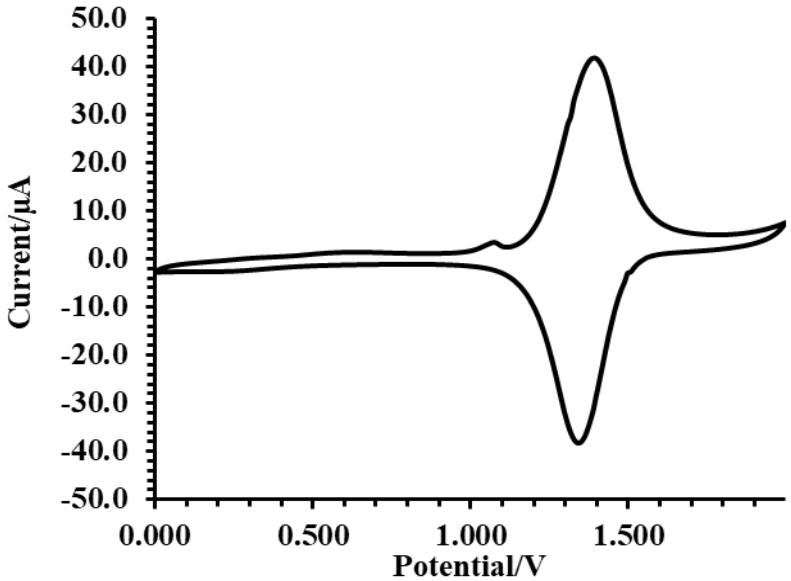

Figure 5. The characterization of the *poly*-Fe(Phen-NH_2)$_3$ film on a glassy carbon electrode in 0.100 M TEAP at 25 mV·s^{-1} using a potential of 0.00 V to 2.00 V vs Ag/AgCl.

Scan rates less than 25 $mV{\cdot}s^{-1}$ produce peak separations of practically 0 V, indicating Nernstian equilibrium with the applied potential; that is, increasing the scan rates causes the peak separation to increase, as semi-infinite diffusion conditions dominate the system, and the cyclic voltammetric scan rate is high relative to the rate of charge transfer. In addition, at scan rates less than 25 $mV{\cdot}s^{-1}$, i_{pa}/i_{pc}=1.00, but the peak width at half-height is greater than the predicted value of 90.4 mV/n, indicating the presence of nonequivalent redox centers and/or attractive or repulsive forces present within the film [25]. The polymer film is essentially a three-dimensional network of redox centers surrounded by solvent pockets devoid of counterions in some areas of the film but present in other locations. Hence, the local activity of the film changes as distance from the electrode surface increases. This also points to the changing activity of $[Fe^{2+}]/[Fe^{3+}]$ as time varies during the cyclic voltammetry scan [26].

Figure 6 shows the characterization of the films on ITO surfaces corresponding to 10 $mV{\cdot}s^{-1}$ and 25 $mV{\cdot}s^{-1}$ scan rates. Using these scan rates, the peak currents increased by a factor of 2.66. A complete plot of the peak currents with respect to the scan rate produced a linear trend, indicating the thin film electrochemistry of the polymer film on the ITO surface. In addition, the $E^{o'}$ values obtained for $Fe^{3+/2+}$ of the films on the ITO surfaces and glassy carbon electrodes are very similar, with ITO films having an $E^{o'}$ value of 1.30 V. The larger current response is a result of the larger surface area of the ITO surface relative to the glassy carbon electrode.

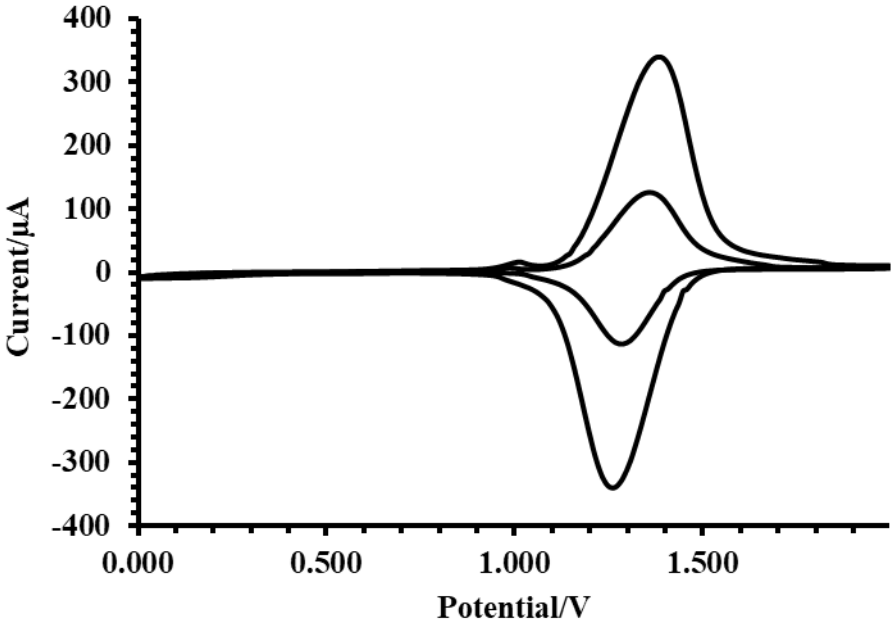

Figure 6. The characterization of a *poly*-Fe(Phen-NH_2)$_3$ film on an ITO surface in 0.100 M TEAP at 25 $mV{\cdot}s^{-1}$ using a potential of 0.00 V to 2.00 V vs Ag/AgCl.

3.4 Spectroelectrochemical and SEM characterization of poly-Fe(Phen-NH_2)$_3$ films.

Spectroelectrochemical measurements in the cyclic voltammetric mode and constant potential mode demonstrate the electrochromic properties of the polymer films on ITO surfaces, switching

between the colors of red and yellow. The overlay spectra obtained after applying potentials of 1.50 V, 1.35 V, 1.30 V, 1.25 V, and 1.20 V are shown in Figure 7. At a potential of 1.50 V, the predominant redox state is Fe^{3+} in the polymer film, and the film is yellow. However, as the potential becomes more negative, an absorption band begins to appear at ca. 506 nm and reaches a maximum absorbance of 0.500 at 1.20 V. At this voltage, the film switches to red, wherein the predominant redox state is Fe^{2+}. An isosbestic point appears at 412 nm, indicating the presence of two principle species, Fe^{2+}/Fe^{3+}, in Nernstian equilibrium and with equal molar absorptivity values. In addition, the cyclic voltammetric characterization shown in Figure 5 also indicates facile electron transfer and Nernstian equilibrium of the Fe^{3+}/Fe^{2+} oxidation states with the applied potential at low scan rates. Using the absorbance values $(A_2\text{-}A_{ox})/(A_{red}\text{-}A_2)$ to plot the applied potential with respect to log [O]/[R] yields an estimation of $E^{o'}$ in 0.100 M TEAP, where A_2 represents an absorbance measurement, and A_{ox} and A_{red} are the absorbance measurements of the oxidized and reduced states, respectively [27]. The equation of the line provided an intercept of 1.31 V, which is $E^{o'}$; this coincides with the $E^{o'}$ value determined by the cyclic voltammetric measurements shown in Figures 5 and 6.

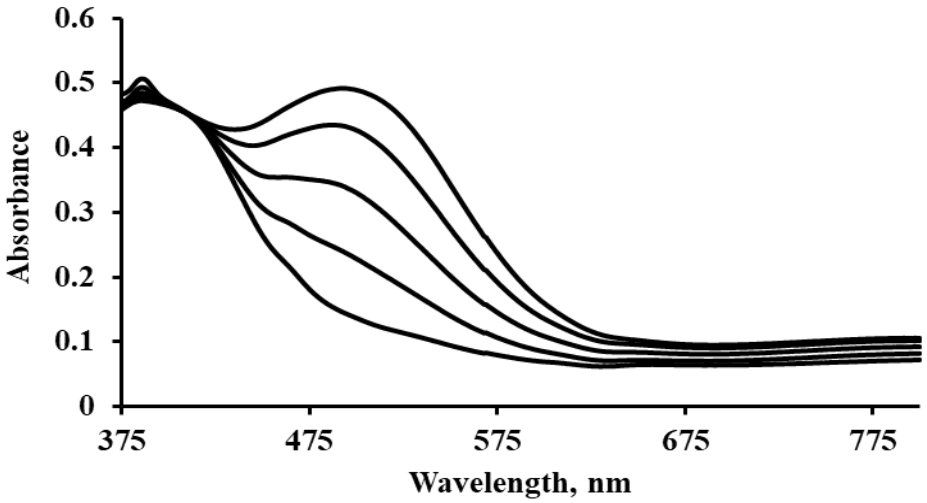

Figure 7. The overlay spectra obtained from the spectroelectrochemical measurements made in the pulsed-potential mode of the *poly*-Fe(Phen-NH_2)$_3$ film in 0.10 M TEAP in acetonitrile. The polymer film is based on twenty cycles of electropolymerization. Applied potentials vs Ag/AgCl from the bottom to the top are 1.50 V, 1.35 V, 1.30 V, 1.25 V, and 1.20 V. A platinum wire served as the auxiliary electrode.

Electrochromic materials can be characterized at a specific wavelength in terms of optical or chromic contrast (ΔT), optical density (ΔOD_λ), and electrochromic or coloration efficiency (CE). These parameters [13, 28] are defined by equations (1)-(3). The optical contrast parameter shown in equation (1) is the difference in the transmittance of the bleached (T_b) state and colored (T_c) state of the polymer film:

$$\Delta T = T_b - T_c \quad (1)$$

The optical density factor at a specific wavelength is given by equation (2):

$$\Delta OD_{\lambda} = \log \frac{T_b}{T_c} \quad (2)$$

The electrochromic or coloration efficiency shown in equation (3) is described by two terms, the optical density and the charge inserted (Q_{in}) per unit area (A) to the initiate the switch in the redox state:

$$CE = \frac{\Delta OD_{\lambda}}{Q_{in}} \quad (3)$$

where the value of Q_{in} was determined by the characterization cyclic voltammogram:

$$Q_{in} = \int \frac{i \, dt}{A} \quad (4)$$

Figure 8a corresponds to the spectroelectrochemical measurements performed at 506 nm using the cyclic voltammetric mode and 0.100 M TEAP as the supporting electrolyte system, wherein the width of each cycle is dependent upon the scan rate. When the film is in the oxidized state ($Fe^{2+} \rightarrow Fe^{3+} + e^-$), the absorbance obtains a minimum value. However, as the potential is made more negative to realize the reduction process ($Fe^{3+} + e^- \rightarrow Fe^{2+}$), the absorbance reaches a maximum. This oscillation continues with little change in the maximum absorbance. Using ΔOD_{λ} and Q_{in} values of 0.575 and 0.487 mC/cm^2, respectively, the electrochromic efficiency is 1180 cm^2/C. These values are based on using 100%ΔT, although some groups have used 95%ΔT. Other research groups have cited electrochromic efficiency values of conjugated polymer systems within the range 500-3000 cm^2/C [29].

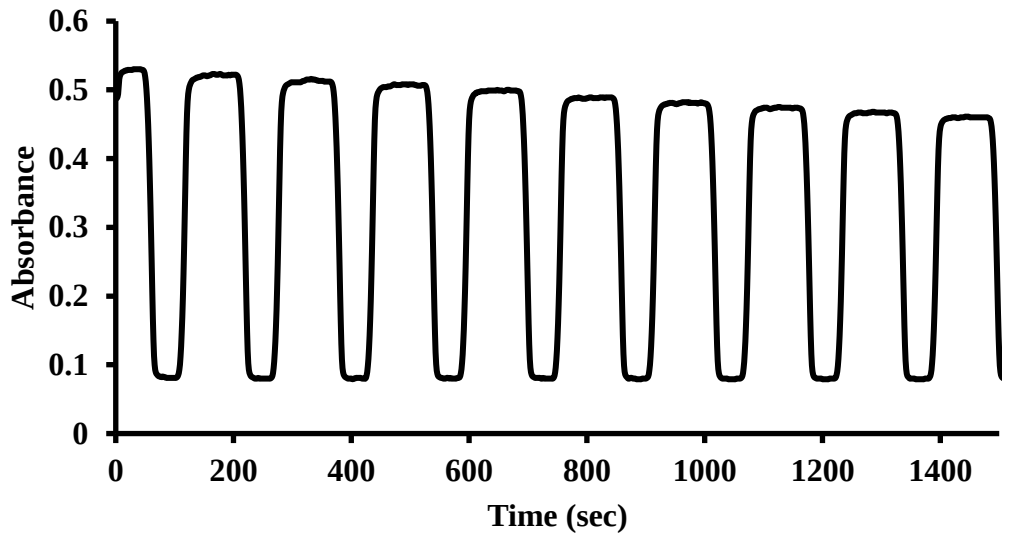

Figure 8a. The spectroelectrochemical characterization of a *poly*-Fe(Phen-NH_2)$_3$ film on an ITO surface measured at 506 nm and 25 mV·s^{-1} vs Ag/AgCl reference electrode in 0.100 M TEAP.

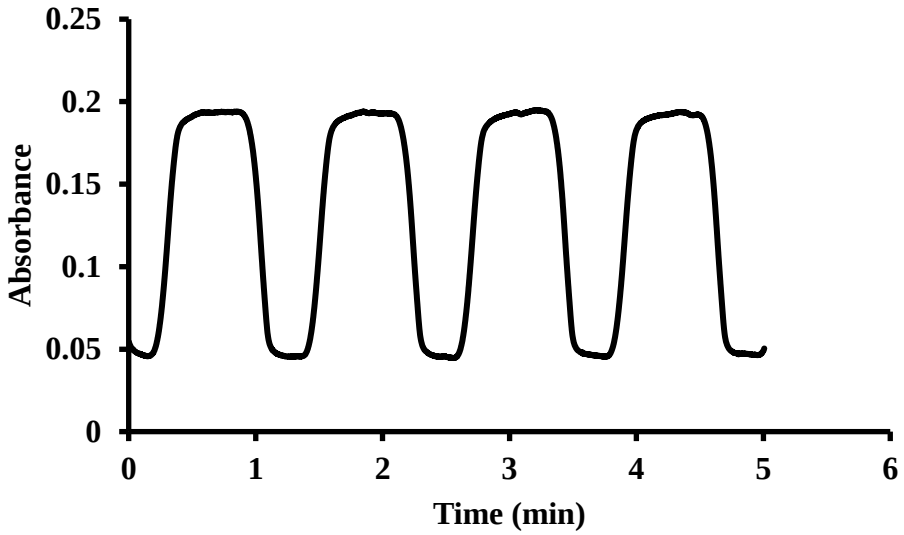

Figure 8b. The spectroelectrochemical characterization of a *poly*-Fe(Phen-NH_2)$_3$ film on an ITO surface measured at 506 nm and 25 mV·s^{-1} vs Ag/AgCl reference electrode in 0.100 M TBAP.

The impact of the supporting electrolyte system on the electrochromic properties of the polymer film was evaluated using 0.100 M TBAP. Upon the reduction of the polymer film, the ClO_4^- counterion is released from the film, or, concomitantly, TEA^+/TBA^+ ingresses into the film. The significantly reduced absorbance, and, hence, the lower electrochromic efficiency shown in Figure 8b for the TBAP-based system are attributed to the difficulty of TBA^+ to provide charge electroneutrality within the polymer film upon redox switching. The counter ion TBA^+ is larger than TEA^+ and hence, the mobility of TBA^+ within the polymer film is lower than TEA^+. Therefore, the diffusion of ions in the polymer film is the limiting factor for the overall electrochromic response of the polymer film. The switching time for the polymer film is dependent upon the ratio, L^2/D, where D is the ionic diffusivity, and L is the film thickness [28]. Hindrances to ionic diffusion within the polymeric network limit the switching time and overall performance of the polymer film as an electrochromic material. The switching times for the reduction and oxidation processes are 3.5 seconds and 7.2 seconds, respectively, based on twenty cycles of electropolymerization.

Figure 9 shows an SEM image obtained with 2500X magnification of a polymer film on an ITO surface undergoing twenty cycles of electropolymerization. The different levels of gray features in the image represent the topographical, structural, and porous characteristics of the polymer film. In addition, the porous nature of the polymer film is indicative of a material that does not form in regular layers during the electropolymerization process, as any solvent pockets present within the film are randomly distributed. No doubt, the redox centers throughout the monolayers are nonequivalent or attractive, or repulsive forces are present [25, 26]; this is confirmed by the broad characterization cyclic voltammogram of Figures 5 and 6. The film thickness was obtained from AFM measurements by averaging the height differences between the ITO surface and the film after scratching the polymer film. The width of the scratch through the film was approximately 20 μm, and the glass substrate was undamaged. The film thickness corresponding to 20 cycles of electropolymerization is 462 ± 45 nm (n=4).

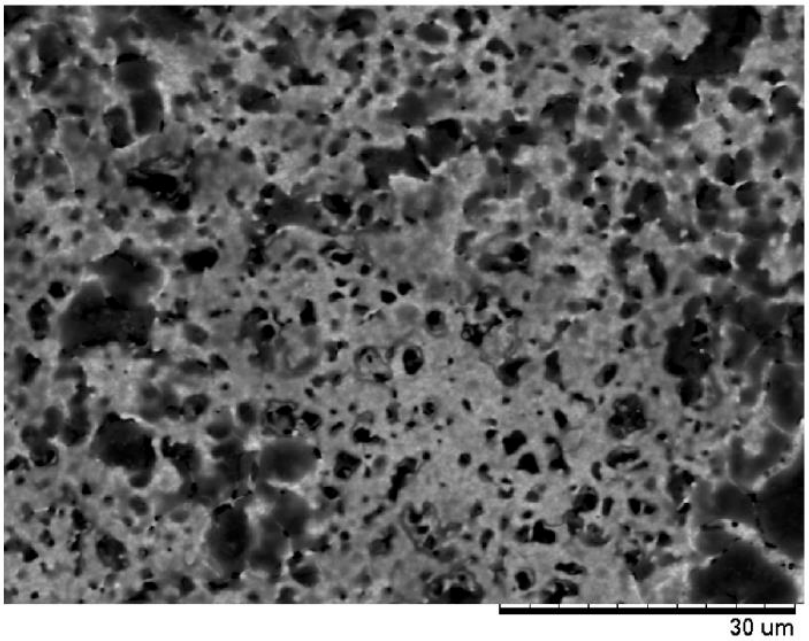

Figure 9. Scanning electron microscopy image obtained at 2500X magnification of a *poly*-Fe(Phen-NH_2)$_3$ film on an ITO surface undergoing twenty cycles of electropolymerization.

3.5 General impedance characterization of poly-Fe(Phen-NH_2)$_3$ films.

Evidence of mixed diffusion and the charge transfer impedances is shown in Figure 10, exhibiting a Nyquist plot of a *poly*-Fe(Phen-NH_2)$_3$ film [13]. The Nyquist plot shows a charge transfer resistance, given by the semicircle at high frequencies of 50000 Hz. Furthermore, at the terminal end of the charge transfer resistance, 181 Hz, a Warburg impedance develops, which results from the diffusion of ions within the polymer film [29]. As the film becomes thicker, the diffusion process becomes anomalous, and the Warburg impedance component deviates from the 45° phase angle [14]. It has been shown that thicker films have a greater surface roughness than thinner films, which leads to the greater trapping of ions. Upon redox switching, there is the possibility that ions become trapped within the shallow or deep regions of the polymer film, which imposes limitations on the optical response of the films [30]. The polymer film can be considered as a structure with dense compact layers closer to the electrode surface and more porous layers near the polymer film|electrolyte interface. Thicker films provide a more porous structure containing solvent pockets with or devoid of ions randomly distributed throughout the polymeric network. More diffusion occurs within the thicker porous structure as the ions have more residence time along the diffusional path segments, giving rise to anomalous diffusion and a Warburg impedance [31]. Characteristically, thinner films also exhibit a Warburg impedance, but with a normal diffusion path and a smaller resistance for charge transfer. No doubt as the electrolyte interacts with the polymer film during redox switching, film swelling occurs, which causes the film structure, the diffusional process, the pathway of ions, and the Warburg impedance to change.

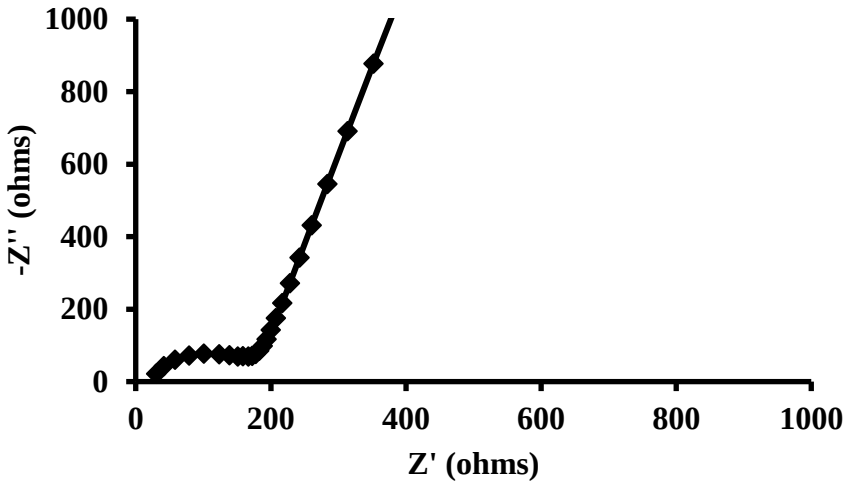

Figure 10. The electrochemical impedance spectroscopy characterization showing the Nyquist plot of the *poly*-Fe(Phen-NH_2)$_3$ film on a glassy carbon electrode in 0.100 M TEAP. The parameters include the following: a 1.30 V DC potential and a 10 mV AC potential amplitude vs Ag/AgCl; 0.001 Hz to 50000 Hz.

Electropolymerized films of Fe(Phen-NH_2)$_3$ have never been characterized using spectroelectrochemical, electrochemical impedance spectroscopy, and microscopy methods to understand the charge transfer processes occurring within these films. The results of characterizing the Fe(Phen-NH_2)$_3$ films on glassy carbon and ITO surfaces with these methods have been correlated to each other. Due to the differences in the spectroelectrochemical response of the films in the TEAP and TBAP supporting electrolyte solutions, the films hold promise as electroactive immobilized reagents in spectroelectrochemical sensors and electrochromic devices. In comparison to other polymer film systems, electropolymerized films of metal(II)-tetraaminophthalocyanine also exhibit similar electrochromic responses when exposed to TEAP and TBAP supporting electrolyte solutions [32]. Furthermore, electrochromic devices that are based on the copolymerization of EDOT and phenylthiophene compounds on ITO surfaces have electrochromic efficiency values ranging from 15.6 - 152 cm^2/C [33]. With EDOT substituents, multiple redox processes can occur, giving rise to various colored states. The cyclic voltammetric response of *poly*-Fe(Phen-NH_2)$_3$ is very similar to that of other ligand systems with iron as the redox center [34]. Iron and ruthenium porphyrin complexes consisting of -amino and -hydroxy substituents have been electropolymerized on glassy carbon and platinum electrodes to prepare multilayered polymer films, which exhibited facile electron hopping between redox centers when characterized using cyclic voltammetry in various supporting electrolyte solutions. In addition, in most of these systems, the peak width at half-height is greater than the predicted 90.4 mV/n value; however, the film thicknesses are not reported [34].

4. CONCLUSIONS

Electropolymerized films of Fe(Phen-NH_2)$_3$ are formed with ease on both glassy carbon electrodes and ITO surfaces and exhibit good electrochemical reversibility at the glassy carbon

electrode. The films are stable upon prolonged electrochemical stimulation in supporting electrolyte solutions and are not removed from glassy carbon or ITO surfaces. The films demonstrate reversible electrochromism that is very comparable to other systems, both organic conducting polymer films and redox films, in terms of efficiency. However, the electrochromic properties, such as a switching time of several seconds, are dependent upon the ion mobility within the polymer films. Although this switching time value is beyond the millisecond time scale, our values are based upon a film thickness greater than 400 nm. Fine tuning the electropolymerization process through a simplex optimization algorithm to better control the film thickness, film charge transfer resistance, and electrochromic response is currently under study.

ACKNOWLEDGMENTS
Research supported by the National Science Foundation-Research Experience for Undergraduates (NSF Grant Award #1263097) and the Hope College Chemistry Department Endowed Funds.

References

1. E. M. Baum, H. Li, T. F. Guarr and J. D. Robertson, *Nucl. Instrum. Methods Phys. Res. B Beam Interact. Mater. At.,* 56-57 (1991) 761.
2. K. L. Brown and H. A. Mottola, *Langmuir*, 14 (1998) 3411.
3. S. W. Feldberg, *J. Am. Chem. Soc.*, 106 (1984) 4671.
4. A. S. Widge, M. Jeffries-El, X. Cui, C. F. Lagenaur and Y. Matsuoka, *Biosens. Bioelectron*., 22 (2007) 1723.
5. S. L. Zelinka, L. Ortiz-Candelaria, D. S. Stone and D. R. Rammer, *Forest Prod. J*., 59 (2009) 77.
6. S. Mondal, T. Yoshida, S. Maji, K. Ariga and M. Higuchi, *ACS Appl. Mater. Interfaces*, 12 (2020) 16342.
7. P. Denisevich, K. W. Willman and R. W. Murray, *J. Am. Chem. Soc*., 103 (1981) 4727.
8. M. Yamada, N. Ohnishi, M. Watanabe and Y. Hino, *Chem. Commun*., 46 (2009) 7203.
9. B. Krische and M. Zagorska, *Synth. Met*., 33 (1989) 257.
10. J. M. Calvert, R. H. Schmehl, B. P. Sullivan, J. S. Facci, T. J. Meyer and R. W. Murray, *Inorg. Chem.*, 22 (1983) 2151.
11. K. Maksymiuk and K. Doblhofer, *Electrochim. Acta*, 39 (1994) 217.
12. S. A. Sapp, G. A. Sotzing and J. R. Reynolds, *Chem. Mater*., 10 (1998) 2101.
13. T. Xu, E. C. Walter, A. Agrawal, C. Bohn, J. Velmurugan, W. Zhu, H. J. Lezec and A. A. Talin, *Nat. Commun.*, 7 (2016) 10479.
14. G. Láng and G. Inzelt, *Electrochim. Acta*, 36 (1991) 847.
15. P. N. Bartlett and K. F. E. Pratt, *J. Electroanal. Chem*., 397 (1995) 61.
16. M. V. Martinez, R. Coneo Rodriguez, A. Baena Moncada, C. R. Rivarola, M. M. Bruno, M. C. Miras and C. A. Barbero, *J. Solid State Electrochem*., 20 (2016) 2951.
17. W. M. F. Nyasulu and H. A. Mottola, *J. Electroanal. Chem. Interfacial Electrochem*., 239 (1988) 175.
18. J. R. Schmidt and W. F. Polik, WebMO Enterprise, Version 20.0, WebMO LLC, (2020) Holland, MI.
19. G. A. Sotzing, J. R. Reynolds and P. J. Steel, *Chem. Mater*., 8 (1996) 882.
20. P. T. Kissenger and W. R. Heineman, Laboratory Techniques in Electroanalytical Chemistry, Marcel Dekker, (1996) New York, NY.
21. A. Akhoury, L. Bromberg and T. A. Hatton, *J. Phys. Chem*. B, 117 (2013) 333.

22. W. Ogieglo, H. Wormeester, K.-J. Eichhorn, M. Wessling and N. E. Benes, *Prog. Polym. Sci*., 42 (2015) 42.
23. J. Troyano, A. Carné-Sánchez, J. Pérez-Carvajal, L. León-Reina, I. Imaz, A. Cabeza and D. Maspoch, *Angew. Chem*., 130 (2018) 15646.
24. M. R. Nateghi, M. H. Mosslemin and H. Hadjimohammadi, *React. Funct. Polym*., 64 (2005) 103.
25. P. Daum, J. R. Lenhard, D. Rolison and R. W. Murray, *J. Am. Chem. Soc*., 102 (1980) 4649.
26. P. Daum and R. W. Murray, *J. Phys. Chem*., 85 (1981) 389.
27. E. L. D'Antonio, E. F. Bowden and S. Franzen, *J. Electroanal. Chem*., 668 (2012) 37.
28. S. Hassab, D. E. Shen, A. M. Österholm, M. Da Rocha, G. Song, Y. Alesanco, A. Viñuales, A. Rougier, J. R. Reynolds and J. Padilla, *Sol. Energy Mater. Sol. Cells*, 185 (2018) 54.
29. M. Fabretto, T. Vaithianathan, C. Hall, J. Mazurkiewicz, P. C. Innis, G. G. Wallace and P. Murphy, *Electrochim. Acta*, 53 (2008) 2250.
30. V. F. Lvovich, Impedance Spectroscopy Applications to Electrochemical and Dielectric Phenomena, Wiley, (2012) New Jersey, NJ.
31. N. Maouche and B. Nessark, Int. J. Electrochem., 2011 (2011) Article ID 670513.
32. H. Li and T. F. Guarr, *J. Electroanal. Chem. Interfacial Electrochem*., 297 (1991) 169.
33. G. R. D. B. S. Lacerda, C. R. Calado and H. D. R. Calado, *J. Solid State Electrochem*., 23 (2019) 823.
34. A. Bettelheim, B. A. White, S. A. Raybuck and R. W. Murray, *Inorg. Chem*., 26 (1987) 1009.

© 2020 The Authors. Published by ESG (www.electrochemsci.org). This article is an open access article distributed under the terms and conditions of the Creative Commons Attribution license (http://creativecommons.org/licenses/by/4.0/).